Contribution from the Department of Chemistry,
University of Toronto, Toronto, Ontario, Canada M5S 1A1

CO Labilization and Hydrogen-Transfer Pathways in Cationic Phosphido-Bridged Re–Pt Heterobimetallic Systems and the Molecular Structures of $[\eta^5\text{-Cp(ON)Re}(\mu\text{-PR}_2)(\mu\text{-H})\text{Pt(PPh}_3)_2]X$ (R = Cy, $X^- = PF_6^-$; R = Ph, $X^- = BF_4^-$) and $[\eta^5\text{-Cp(ON)HRe}(\mu\text{-PCy}_2)\text{Pt(PPh}_3)_2]BF_4$, a Rare Example of Bridging- and Terminal-Hydrido Geometric Isomers

John Powell,* Jeffery F. Sawyer, and Matthew V. R. Stainer

Received February 29, 1988

Oxidative addition of the cationic secondary phosphine complexes $[\eta^5\text{-Cp(OC)(ON)Re(PR}_2\text{H)}]^+$ (**6**) (R = Ph, Cy, Pr) to $Pt(C_2H_4)(PPh_3)_2$ gives $[\eta^5\text{-Cp(OC)(ON)Re}(\mu\text{-PR}_2)\text{PtH(PPh}_3)_2]^+$ (**7**). In contrast, reaction of **6** with $Pt(PPh_3)_4$ leads to CO loss and the formation of the terminal rhenium hydride derivative $[\eta^5\text{-Cp(ON)HRe}(\mu\text{-PR}_2)\text{Pt(PPh}_3)_2]^+$ (**8**) as the kinetic product. On standing, **8** slowly transforms into the thermodynamically preferred bridging-hydrido isomer $[\eta^5\text{-Cp(ON)Re}(\mu\text{-PR}_2)(\mu\text{-H})\text{-Pt(PPh}_3)_2]^+$ (**9**). The cations **7** will undergo slow CO loss to form **8** in the presence of base (e.g. F^-, proton sponge), and the isomerization of **8** to **9** is promoted by added chloride ion with $-d[\mathbf{8}]/dt = k[\mathbf{8}][Cl^-]^2$. Complex **7** (R = Cy) reacts with added Cl^- to give $[\eta^5\text{-Cp(OC)(ON)Re}(\mu\text{-PCy}_2)\text{PtHCl(PPh}_3)]$ (**10b**), which reacts with Cl^- abstractors (Ag^+ or $NaBPh_4$) to give an equilibrium mixture of $[\eta^5\text{-Cp(ON)Re}(\mu\text{-PCy}_2)(\mu\text{-H})\text{Pt(PPh}_3)(CO)]^+$ (**11b**) and $[\eta^5\text{-Cp(ON)HRe}(\mu\text{-PCy}_2)\text{Pt(PPh}_3)(CO)]^+$, (**12b**) ($PPh_3$ trans to μ-PCy_2), which slowly transform to give $[\eta^5\text{-Cp(ON)HRe}(\mu\text{-PCy}_2)\text{Pt(PPh}_3)(CO)]^+$ (**13b**) (PPh_3 cis to μ-PCy_2). Cations **12b** and **13b** react rapidly with PPh_3 to give **8** while **11b** reacts with PPh_3 to give **9b**. The mechanism of formation of **7** and **8** from **6** and the mechanism of the base-promoted **7** to **8** rearrangement and the Cl^--catalyzed **8** to **9** isomerization process are discussed. The molecular structures of $[\eta^5\text{-Cp(ON)HRe}(\mu\text{-PCy}_2)\text{Pt(PPh}_3)_2]BF_4$ ((**8b**)BF_4) and $[\eta^5\text{-Cp(ON)Re}(\mu\text{-PCy}_2)(\mu\text{-H})\text{Pt(PPh}_3)_2]PF_6$ ((**9b**)PF_6) (a rare example of terminal- and bridging-hydrido isomers) and $[\eta^5\text{-Cp(ON)Re}(\mu\text{-PPh}_2)(\mu\text{-H})\text{Pt-(PPh}_3)_2]BF_4$ ((**9a**)BF_4) have been determined. Crystal data for (**8b**)BF_4: $C_{53}H_{58}BF_4NOP_3PtRe\cdot CH_2Cl_2$ crystallizes in space group $P2_1/n$ with a = 11.031 (2) Å, b = 22.391 (5) Å, c = 21.603 (7) Å, β = 94.04 (2)°, V = 5322 Å^3, and Z = 4. The structure was refined to R = 0.0407 and R_w = 0.0419. Crystal data for (**9a**)BF_4: $C_{53}H_{46}BF_4NOP_3PtRe$, space group $P\bar{1}$ with a = 12.563 (2) Å, b = 12.896 (1) Å, c = 15.024 (2) Å, α = 94.14 (1)°, β = 96.93 (2)°, γ = 92.01 (1)°, V = 2407 Å^3, and Z = 2. The structure was refined to R = 0.0310 and R_w = 0.0325. Crystal data for (**9b**)PF_6: $C_{53}H_{58}F_6NOP_4PtRe\cdot 2.5CH_2Cl_2$, space group $P\bar{1}$, a = 12.532 (2) Å, b = 13.077 (2) Å, c = 19.101 (2) Å, α = 94.85 (1)°, β = 105.40 (1)°, γ = 91.23 (1)°, V = 3004 Å^3, and Z = 2. The structure was refined to R = 0.0471 and R_w = 0.0508. Cations **9a** and **9b** contain a planar "$Re(\mu\text{-PR}_2)(\mu\text{-H})Pt$" unit, the bridging hydrogen atom being located in both structures from difference Fourier maps, refined by least squares. The cation **8b** contains a planar "$HRe(\mu\text{-PCy}_2)Pt$" unit. The position of the terminal hydride is inferred to be bonded to Re (confirmed by ^1H NMR) in a position approximately trans to the Pt–Re bond by using (i) the approach of Orpen for the calculation of minimization of van der Waals repulsion energies and (ii) EHMO calculations. In contrast to previous studies a good correlation between $^1J_{^{195}Pt-^{31}P}$ and Pt–P bond lengths is observed for the complexes **8b**, **9a**, and **9b**.

Introduction

Oxidative addition of the P–H bond of a secondary-phosphine complex to zerovalent complexes of platinum provides easy access to singly bridged μ-phosphido heterobimetallic hydrides.[1-5] Because of the available stereochemical signposting (^1H, ^{13}C, ^{31}P, and ^{195}Pt NMR; ν(CO), IR) these systems are particularly suitable for (i) the study of cluster assembly and cluster rearrangement processes, (ii) the study of ligand reactivities in multimetallic systems and (iii) an analysis of the way(s) in which the chemistry of one metal center may be modified by a second metal center in close proximity. Thus for example the group VI metal carbonyl complexes $M(CO)_5(PPh_2H)$ (**1**) (M = Cr, Mo, W) oxidatively add to $Pt(C_2H_4)(PPh_3)_2$ to give the μ-phosphido bimetallic complex $(OC)_5M(\mu\text{-PPh}_2)\text{PtH(PPh}_3)_2$ (**2**).[1,5] This complex loses CO under very mild conditions (for a group VI carbonyl)[6] to give the μ-phosphido–μ-hydrido complex $(OC)_4M(\mu\text{-PPh}_2)(\mu\text{-H})\text{Pt(PPh}_3)_2$ (**3**). While the net result of this reaction is effectively a substitution of CO at M by H, the reaction proceeds by a platinum-assisted process involving PPh_3 dissociation from Pt and CO transfer via $(OC)_4M(\mu\text{-PPh}_2)(\mu\text{-CO})\text{PtH(PPh}_3)$, to give the ($\mu$-hydrido)-platinum carbonyl $(OC)_4M(\mu\text{-PPh}_2)(\mu\text{-H})\text{Pt(CO)(PPh}_3)$ (**5**), followed by displacement of CO from Pt by PPh_3 (see preceding paper[5]). The success of this approach to the synthesis of μ-phosphido bimetallics is sensitive to both the acidity of the P–H bond and steric effects.[5,7] Thus substitution of a carbonyl ligand by a donor phosphine to give $M(CO)_4(PR_3)(PR_2H)$ (increased sterics and decreased acidity) or replacement of PPh_2H with PCy_2H in $M(CO)_5(PR_2H)$ markedly retards the oxidative-addition step. To overcome this problem of low reactivity and to obtain μ-phosphido complexes with a range of ligands other than strongly electron-withdrawing carbonyls, we have chosen to synthesize and investigate the reactions of a series of *cationic* secondary phosphine complexes since in these systems the overall positive charge provides for increased acidity of the P–H bond, thereby facilitating oxidative addition.[2,3]

In this paper, we report the results pertaining to the reactions of the cationic rhenium secondary-phosphine complexes $[Cp(ON)(OC)Re(PR_2H)]^+X^-$ ((**6**)X) (R = Ph, Cy, ^{n}Pr; $X^- = BF_4^-$, BPh_4^-) with $Pt(C_2H_4)(PPh_3)_2$, $Pt(PPh_3)_4$, and $Pt(C_2H_4)_2(PCy_3)$. The study of these and structurally similar rhenium–platinum systems provide evidence of a second reaction pathway for "platinum-assisted CO substitution" in which proton-transfer phenomena play a significant role in determining the structure of the reaction products. X-ray structural studies of the isomeric

(1) Powell, J.; Gregg, M. R.; Sawyer, J. F. *J. Chem. Soc., Chem. Commun.* **1984**, 1149.
(2) Powell, J.; Sawyer, J. F.; Smith, S. J. *J. Chem. Soc., Chem. Commun.* **1985**, 1312.
(3) Powell, J.; Sawyer, J. F.; Stainer, M. V. R. *J. Chem. Soc., Chem. Commun.* **1985**, 1314.
(4) Powell, J.; Gregg, M. R.; Sawyer, J. F. *J. Chem. Soc., Chem. Commun.* **1987**.
(5) Powell, J.; Gregg, M. R.; Sawyer, J. F. *Inorg. Chem.*, preceding paper in this issue.
(6) Darensbourg, D. J. *Adv. Organomet. Chem.* **1982**, *21*, 112.
(7) Guggenberger, L. S.; Klabunde, U.; Schunn, R. A. *Inorg. Chem.* **1973**, *12*, 1143.

0020-1669/89/1328-4461$01.50/0 © 1989 American Chemical Society

Table I. IR and ^1H NMR Data for the Complexes $[\eta^5\text{-Cp(ON)(OC)Re}(\mu\text{-PR}_2)\text{PtH(PPh}_3)_2]^+$ (**7a–c**), $[\eta^5\text{-Cp(ON)}\overline{\text{HRe}(\mu\text{-PR}_2)}\text{Pt(PPh}_3)_2]^+$ (**8a–c**), $[\eta^5\text{-Cp(ON)Re}(\mu\text{-PR}_2)(\mu\text{-H})\text{Pt(PPh}_3)_2]^+$ (**9a–c**), $[\eta^5\text{-Cp(ON)(OC)Re}(\mu\text{-PCy}_2)\text{PtHCl(PPh}_3)]$ (**10b**), $[\eta^5\text{-Cp(ON)Re}(\mu\text{-PCy}_2)(\mu\text{-H})\text{Pt(CO)(PR}_3)]^+$ (**11b** (PR_3 = PPh_3), **17b** (PR_3 = PCy_3)), $[\eta^5\text{-Cp(ON)}\overline{\text{HRe}(\mu\text{-PCy}_2)}\text{Pt(CO)(PPh}_3)]^+$ (**12b** (PPh_3 trans to PCy_2), **13b** (PPh_3 cis to PCy_2)), $[\eta^5\text{-Cp(ON)Re}(\mu\text{-PCy}_2)(\mu\text{-CO})\text{PtH(PCy}_3)]^+$ (**16b**)

		IR data, cm^{-1}		^1H NMR data[d] (δ, ppm; J, Hz)					
				δ(H)					
complex	μ-PR_2	ν(CO)	ν(NO)	η^5-Cp	hydrido ligand	$J_{P_\mu\text{-H}}$	$J_{^{31}P_c\text{-}^1H}$	$J_{^{31}P_t\text{-}^1H}$	$J_{^{195}Pt\text{-}^1H}$
7a[a]	PPh_2	1994	1741	5.28	−5.92	18	27	165	854
7b[b]	PCy_2	1994	1738	5.55	−6.91	17	19	163	807
7c[b]	P^nPr_2	1995	1738	5.57	−6.08	17	21	165	874
8a[a]	PPh_2		1702	4.82	−7.45	31	7	3	36
8b[b]	PCy_2		1705	5.13	−7.72	34	7	0	40
8c[b]	P^nPr_2		1705	5.00	−8.13	33	7	2	36
9a[a]	PPh_2		1687	4.74	−3.01	29	7	52	404
9b[b]	PCy_2		1682	5.05	−3.00	30	7	56	432
9c[b]	P^nPr_2		1686	4.94	−3.02	29	7	53	409
10b	PCy_2	1988	1717	5.92	−17.51	11	14		1308
11b[b]	PCy_2	2073[c]	1711	5.21	−3.49	29	4		506
12b[b]	PCy_2	2060[c]	1709	5.16	−7.15	34	10		50
13b[b]	PCy_2	2059[c]	1725	6.01	−6.54	33		0	38
16b[b]	PCy_2	1800	1733	5.91	−1.80	20	20		1110
17b[b]	PCy_2	2067[c]	1703	5.62	−4.5	23	5		542

[a] BF_4^- salts. [b] BPh_4^- salts. [c] CO (coordinated to Pt). [d] P_μ bridging; P_c cis to and P_t trans to the H or RePt bond.

Table II. $^{31}P\{^1H\}$ NMR Data (δ, ppm; J, Hz) (CD_2Cl_2) for the Complexes **7–13**, **16**, and **17**[a]

	$\delta(P_\mu)$	$\delta(P_c)$	$\delta(P_t)$	$J_{P_\mu\text{-}P_c}$	$J_{P_\mu\text{-}P_t}$	$J_{P_c\text{-}P_t}$	$J_{^{195}Pt\text{-}P_\mu}$	$J_{^{195}Pt\text{-}P_c}$	$J_{^{195}Pt\text{-}P_t}$
7a	−42.1	19.7	24.4	323	18	15	2185	2580	2153
7b	−10.8	15.9	26.1	288	16	19	2190	2350	2210
7c	−5.3	19.6	23.7	306	19	18	2140	2368	2198
8a	147.2	24.0	24.6	255	11	9	2308	3017	3543
8b	200.2	23.7	23.8	224	8	6	2131	2842	3591
8c	153.8	22.0	21.5	235	7	4	2101	2892	3583
9a	128.7	12.7	20.1	229	9	26	1998	2583	4153
9b	167.7	10.3	19.3	199	8	26	1777	2366	4270
9c	132.9	10.6	19.2	208	9	24	1810	2448	4209
10b	AB and ABX patterns: $\delta(P_A)$ = 17.3, $\delta(P_B)$ = 30.3; J_{AB} = 364 Hz, J_{AX} = 2417 Hz, J_{BX} = 2671								
11b	185.6	13.2		161			1453	2445	
12b	207.1	21.4		187			1841	2778	
13b	193.7		22.1		12		2362		3386
16b	184.5	41.3		166			1140	3226	
17b	173.0	31.8		150			1287	2370	

[a] See Table I. Key: P_μ, bridging phosphido; P_c, PR_3 ligand cis to the H or RePt bond; P_t, PR_3 ligand trans to the H or RePt bond.

cationic terminal-hydride $[Cp(ON)\overline{HRe(\mu\text{-}PCy_2)}Pt(PPh_3)_2]^+$ and the bridging-hydride analogues $[Cp(ON)Re(\mu\text{-}PR_2)(\mu\text{-}H)Pt(PPh_3)_2]^+$ (R = Cy, Ph) are presented, and the mechanism of the terminal- to bridging-hydrido isomerization is shown to be catalyzed by halide ions. A preliminary account of this work has been presented.[3]

Results

Reaction of $[Cp(OC)(ON)Re(PR_2H)]^+$ with $Pt(C_2H_4)(PPh_3)_2$ and $Pt(PPh_3)_4$. The cationic secondary-phosphine complexes $[Cp(OC)(ON)Re(PR_2H)]^+$ (R = Ph (**6a**), Cy (**6b**), ^{n}Pr (**6c**)) were prepared by following the method of Tam et al.[8] for the synthesis of $[Cp(OC)(ON)Re(PPh_3)]^+$ as outlined in eq 1. Complex **6a**

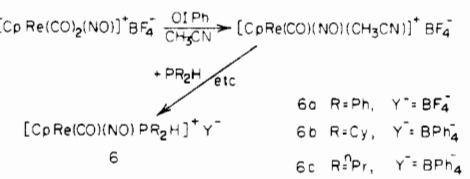

(1)

was prepared and isolated as the BF_4^- salt, while **6b** and **6c** were prepared initially as the BF_4^- salts and then converted to BPh_4^- salts to facilitate purification and crystallization.

In CH_2Cl_2, the complexes **6b,c** react cleanly with $Pt(C_2H_4)(PPh_3)_2$ to produce the cationic (μ-phosphido)platinum hydrides

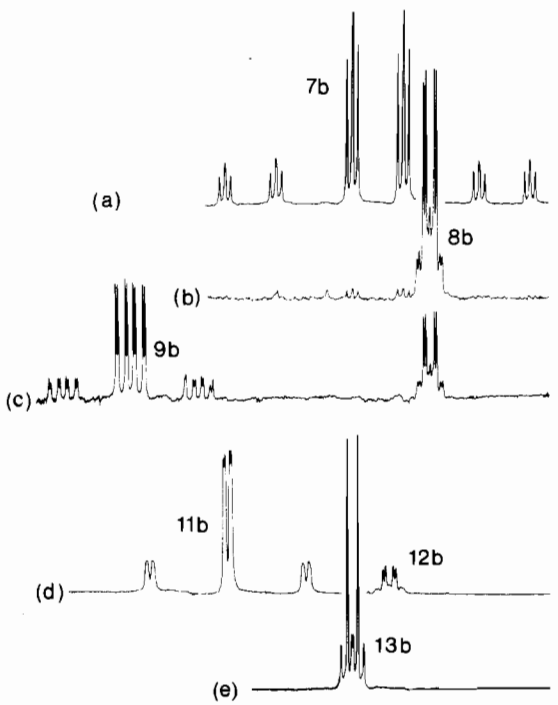

Figure 1. High-field hydridic ^1H NMR spectra (CD_2Cl_2 solution, 20 °C): (a) $[\eta^5\text{-Cp(OC)(ON)Re}(\mu\text{-PCy}_2)\text{PtH(PPh}_3)_2]^+$ (**7b**); (b) $[\eta^5\text{-Cp(ON)}\overline{\text{HRe}(\mu\text{-PCy}_2)}\text{Pt(PPh}_3)_2]^+$ (**8b**); (c) $[\eta^5\text{-Cp(ON)Re}(\mu\text{-PCy}_2)(\mu\text{-H})\text{Pt(PPh}_3)_2]^+$ (**9b**) formed from **8b** after standing in solution at room temperature for ca. 8 days; (d) equilibrium mixture of $[\eta^5\text{-Cp(ON)Re}(\mu\text{-PCy}_2)(\mu\text{-H})\text{Pt(CO)(PPh}_3)]^+$ (**11b**) and $[\eta^5\text{-Cp(ON)}\overline{\text{HRe}(\mu\text{-Cy}_2)}\text{Pt(CO)(PPh}_3)]^+$ (**12b**) (PPh_3 trans to μ-PCy_2); (e) $[\eta^5\text{-Cp(ON)}\overline{\text{HRe}(\mu\text{-PCy}_2)}\text{Pt(CO)(PPh}_3)]^+$ (**13b**) (CO trans to μ-PCy_2).

$[Cp(OC)(ON)Re(\mu\text{-}PR_2)PtH(PPh_3)_2]^+$ (**7b,c**) (eq 2). The

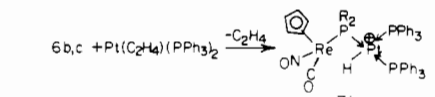

(2)

complexes **7b,c** have been characterized by ^1H and $^{31}P\{^1H\}$ NMR and IR spectroscopy (Figure 1a, Tables I and II) with features fully consistent with the structure shown.[9] The ^1H and $^{31}P\{^1H\}$ NMR data for **7** are very similar to those reported for $[PtH(PR_3)_3]^+$ systems,[10] which suggests that much of the positive charge of **7** may be located on the "P_3PtH" fragment, consistent with the $Re^I(\mu\text{-}PR_2)Pt^{II}$ formulation shown. [N.B. On going from

(8) Tam, W.; Lin, G.-Y.; Wong, W.-K.; Kiel, W. A.; Wong, V. K.; Gladysz, J. A. *J. Am. Chem. Soc.* **1982**, *104*, 141.

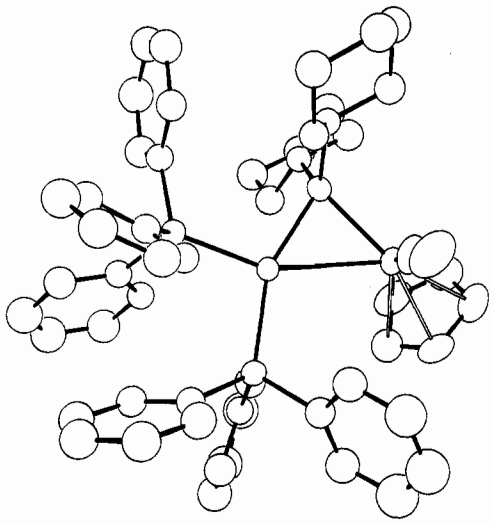

Figure 2. Molecular structure of $[\eta^5\text{-Cp(ON)HRe}(\mu\text{-PCy}_2)\text{Pt(PPh}_3)_2]\text{BF}_4$ ((**8b**)BF_4) as determined by single-crystal X-ray diffraction.

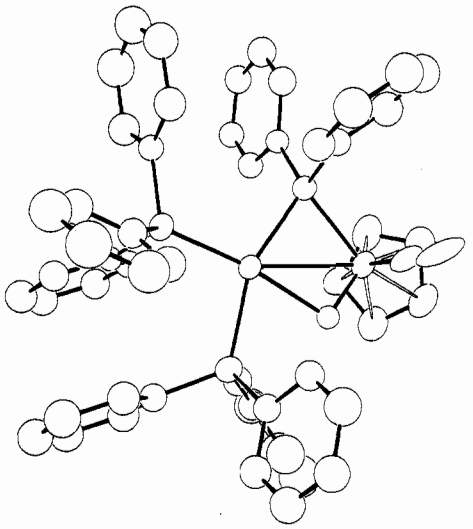

Figure 3. Molecular structure of $[\eta^5\text{-Cp(ON)Re}(\mu\text{-PPh}_2)(\mu\text{-H})\text{Pt(PPh}_3)_2]\text{BF}_4$ ((**9a**)BF_4) as determined by single-crystal X-ray diffraction.

6 to **7**, ν(CO) and ν(NO) decrease by ca. 30 and 22 cm^{-1}, respectively, consistent with removal of positive charge from Re]. Formation of the cis isomer (at Pt), **7**, rather than the trans isomer is presumably a consequence of the large steric bulk (cone angle) of the "Cp(OC)(ON)RePR$_2$" ligand. The reaction between $[Cp(OC)(ON)Re(PPh_2H)]^+$ (**6a**) and $Pt(C_2H_4)(PPh_3)_2$ in CH_2Cl_2 is slightly more complex than eq 2 and is described later.

The reaction of the cations $[Cp(OC)(ON)Re(PR_2H)]^+$ (**6a–c**) with $Pt(PPh_3)_4$ in CH_2Cl_2 results in loss of CO and formation of the terminal rhenium hydrido cations $[Cp(ON)HRe(\mu\text{-PR}_2)Pt(PPh_3)_2]^+$ (**8a–c**) as the major product (eq 3). Besides **8a–c**, there

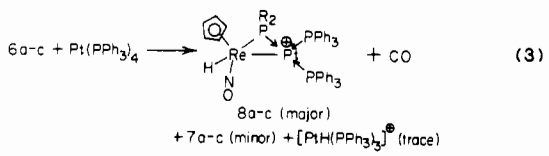

is also formed a minor amount of the cis hydridoplatinum cation (ca. 20% **7b** and **7c**; 5% **7a**) together with a trace of $[PtH(PPh_3)_3]^+$, which is readily identified by its characteristic ^1H and $^{31}P\{^1H\}$ NMR spectra.[10] The molecular structure of the μ-dicyclohexylphosphido derivative (**8b**) as determined by X-ray diffraction is shown in Figure 2. (A detailed discussion of the structural features of **8b** is given later.) Upon standing in CH_2Cl_2 solution (ca. 20 °C), the terminal rhenium hydrido cations $[Cp(ON)HRe(\mu\text{-PR}_2)Pt(PPh_3)_2]^+$ (**8a–c**) slowly rearrange to the bridging-hydrido isomers $[Cp(ON)Re(\mu\text{-PR}_2)(\mu\text{-H})Pt(PPh_3)_2]^+$ (**9a–c**) (eq 4). For **8a** and **8c**, the isomerization to **9** occurs in

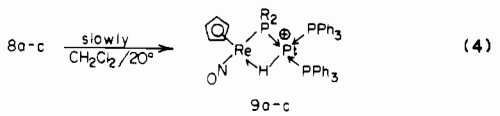

a period of a few hours. Thus although **8a** and **8c** are produced in high yield from **6a**,**c** and $Pt(PPh_3)_4$, they cannot be isolated in the pure form. In contrast to **8b** and **9b** isomerization is much slower for the μ-dicyclohexylphosphido system. In CH_2Cl_2 at −15 °C conversion of **8b** to **9b** (eq 4) is less than 25% over a period of 1 month. The cation $[Cp(ON)HRe(\mu\text{-PCy}_2)Pt(PPh_3)_2]^+$ (**8b**) can be purified on a small scale by column chromatography, and crystals of the tetrafluoroborate suitable for X-ray diffraction studies were obtained from CH_2Cl_2/hexane (see below and Figure 2). The molecular structures of the bridged-hydrido cations **9a** and **9b**, as determined by single-crystal X-ray diffraction studies, are shown in Figures 3 and 4.

The reaction of $[Cp(OC)(ON)Re(PPh_2H)]^+$ (**6a**) with Pt-

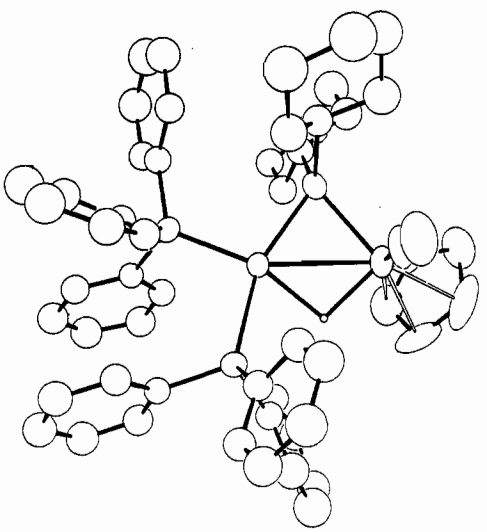

Figure 4. Molecular structure of $[\eta^5\text{-Cp(ON)Re}(\mu\text{-PCy}_2)(\mu\text{-H})\text{Pt(PPh}_3)_2]\text{PF}_6$ ((**9b**)PF_6) as determined by single-crystal X-ray diffraction.

$(C_2H_4)(PPh_3)_2$ in CH_2Cl_2 is more complex than that observed for **6b** and **6c** (see above and eq 2). The course of the reaction and the distribution of products is dependent on the reaction conditions (eq 5). If **6a** is maintained in excess during the mixing of the

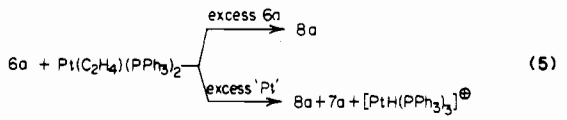

reactants, then the terminal rhenium hydride $[Cp(ON)HRe(\mu\text{-PPh}_2)Pt(PPh_3)_2]^+$ (**8a**) is obtained as the major product (>90%). Alternatively, when **6a** and $Pt(C_2H_4)(PPh_3)_2$ are mixed so that the latter is maintained in excess during the reaction, a mixture containing **8a** (ca. 70%), the terminal platinum hydride $[Cp(OC)(ON)Re(\mu\text{-PPh}_2)PtH(PPh_3)_2]^+$ (**7a**) (ca. 20%), and a small amount of $PtH(PPh_3)_3^+$ (ca. 10%) is obtained. When this mixture is allowed to stand the characteristic ^1H and $^{31}P\{^1H\}$ NMR signals of **8a** decrease and those of **9a** grow, consistent with **8a** and **9a** isomerization. In contrast, the signals of **7a** remain unchanged in intensity, indicating that **7a** does not readily lose CO to give either **8a** or **9a**. Similarly, solutions of the (μ-dipropylphosphido)platinum hydride **7c** are stable with respect to CO loss. No conversion of **7c** to either **8c** or **9c** is observed when solutions of **7c** are allowed to stand at room temperature for several days. Attempts to catalyze the conversion of **7c** to either **8c** or **9c** by the addition of base were unsuccessful.

In contrast to the lack of reactivity with respect to CO loss exhibited by **7a** and **7c**, the μ-dicyclohexylphosphido analogue $[Cp(OC)(ON)Re(\mu\text{-PCy}_2)PtH(PPh_3)_2]^+$ (**7b**) undergoes slow

(9) Moore, D. S.; Robinson, S. D. *Chem. Soc. Rev.* **1983**, *12*, 415.
(10) Dingle, T. W.; Dixon, K. *Inorg. Chem.* **1974**, *13*, 847.

decomposition in CH_2Cl_2 solution to give a mixture containing $[Cp(ON)HRe(\mu\text{-}PCy_2)Pt(PPh_3)_2]^+$ (**8b**) and $[Cp(OC)(ON)Re(PCy_2H)]^+$ (**6b**). Conversion of the platinum hydride **7b** to the rhenium hydride **8b** can be effected more rapidly and with very little formation of **6b** by the addition of base [e.g. F^-, NEt_3 and proton sponge (1,8-bis(dimethylamino)naphthalene)] (eq 6).

$$\mathbf{7b} \xrightarrow{+F^-;\ -CO\uparrow} \mathbf{8b} \tag{6}$$

[N.B. When the same sample is maintained continually in the IR sample cell, **6b** and $Pt(CO)_2(PPh_3)_2$[11] are also formed, presumably via CO capture (see eq 7)]. The relative effectiveness

$$\mathbf{8b} + CO \rightarrow \mathbf{6b} + Pt(CO)_2(PPh_3)_2 \tag{7}$$

of the base-catalyzed conversion of **7b** to **8b** is $F^- > NEt_3 \geq$ proton sponge. (F^- has been previously shown to be particularly effective at deprotonating the sterically restricted cationic hydride $[Mo(CO)_2(Ph_2PCH_2CH_2PPh_2)_2H]^+$.[12]) The addition of base will also effect the conversion of **7a** to **8a**. It should also be noted that the addition of proton sponge to **6a** gives a solution containing $[Cp(OC)(ON)RePPh_2]$ (ν(CO) 1983 cm^{-1}; ν(NO) 1712 cm^{-1}) and [proton sponge H]$^+$. Addition of $Pt(C_2H_4)(PPh_3)_2$ to this solution gives $[Cp(ON)HRe(\mu\text{-}PPh_2)Pt(PPh_3)_2]^+$ (**8a**) as the sole product (i.e. no **7a** is formed). In contrast, **6b** and **6c** are not deprotonated by proton sponge, indicative of a less acidic P–H bond in **6b** and **6c** vis-a-vis **6a**. Bubbling CO through a solution of **8b** gives **6b** and $Pt(CO)_2(PPh_3)_2$ (eq 7). Under similar conditions, the bridging-hydrido isomers **9a–c** do not react with CO (eq 8).

$$\mathbf{9b} + CO \rightarrow \text{no reaction} \tag{8}$$

Synthesis and Reactions of $Cp(ON)(OC)Re(\mu\text{-}PCy_2)PtHCl(PPh_3)$. To obtain further information of possible relevance with regard to the mechanism for the formation of $[Cp(ON)HRe(\mu\text{-}PR_2)Pt(PPh_3)_2]^+$ (**8**) from **6** and $Pt(PPh_3)_4$ and the mechanisms for the rearrangements of $[Cp(OC)(ON)Re(\mu\text{-}PR_2)PtH(PPh_3)_2]^+$ (**7**) into **8**, and **8** into $[Cp(ON)Re(\mu\text{-}PR_2)(\mu\text{-}H)Pt(PPh_3)_2]^+$ (**9**), the neutral hydridochloroplatinum–rhenium bimetallic complex $Cp(ON)(OC)Re(\mu\text{-}PCy_2)PtHCl(PPh_3)$, (**10b**) was synthesized from the reaction of **7b** with chloride (added as $[AsPh_4]Cl$) (eq 9). Reaction of **10b** with the chloride-abstracting

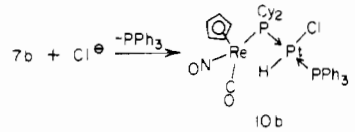

10b (9)

agent $AgBF_4$ in CH_2Cl_2 gave a mixture of metal–metal-bonded and bridging-hydrido species. The reaction was monitored by ^1H and $^{31}P\{^1H\}$ NMR (after removal of AgCl and excess $AgBF_4$). Initially a mixture of $[Cp(ON)Re(\mu\text{-}PCy_2)(\mu\text{-}H)Pt(CO)(PPh_3)]^+$ (**11b**) and $[Cp(ON)HRe(\mu\text{-}PCy_2)Pt(CO)(PPh_3)]^+$ (**12b**) is observed (Figure 1d and eq 10). Complexes **11b** and **12b** can be

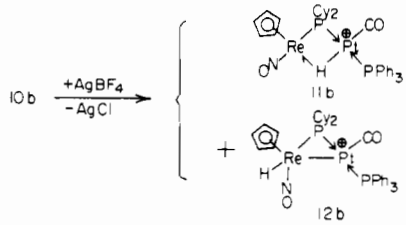

(10)

considered to be derivatives of **9b** and **8b**, respectively. The ν(CO) values of 2073 (**11b**) and 2060 cm^{-1} (**12b**) are comparable to that of *trans*-$[PtH(CO)(PEt_3)_2]^+$ (ν(CO)/2064 cm^{-1})[13] and suggest that much of the positive charge in these cations is located in the Pt region. The relative amounts of **11b** and **12b** observed in the reaction of **10b** with $AgBF_4$ (eq 10) are in the ratio ca. 4:1. Over a period of several days, **11b** and **12b** isomerize (a trans to cis rearrangement of P-donor ligands at Pt) to give the thermodynamically preferred terminal rhenium hydride $[Cp(ON)HRe(\mu\text{-}PCy_2)Pt(PPh_3)(CO)]^+$ (**13b**) (eq 11) (see Figure 1e and Tables

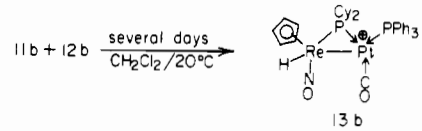

(11)

I and II for spectroscopic data). During the isomerization, the relative ratio of **11b**:**12b** remains constant (as determined by ^1H NMR), suggesting that the **11b**:**12b** ratio is the equilibrium ratio. The isomerization to **13b**, as observed by NMR, is not clean. Minor resonances that can be assigned to $[Cp(ON)Re(\mu\text{-}PCy_2)(\mu\text{-}H)Pt(PPh_3)_2]^+$ (**9b**) and tentatively to the terminal-hydrido platinum species $[Cp(OC)(ON)Re(\mu\text{-}PCy_2)PtH(CO)(PPh_3)]^+$ (**14b**) are also observed. (**14b** presumably arises from

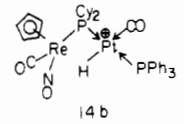

14b

CO capture by **7b**.) IR monitoring of the reaction of **10b** with the chloride-abstracting agent $NaBPh_4$ in acetone solution reveals the formation of a short-lived intermediate $[Cp(ON)Re(\mu\text{-}PCy_2)(\mu\text{-}CO)PtH(PPh_3)]^+$ (**15b**) on the route to **11b** (eq 12). The

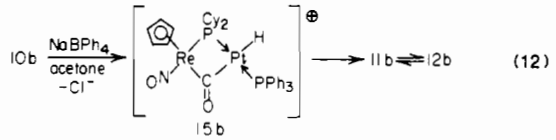

15b (12)

intermediate **15b** is characterized solely on the observed IR absorptions at 1810 cm^{-1}, assigned to a bridging or semibridging carbonyl ligand, and 1740 cm^{-1}, ν(NO). From the IR experiment with $NaBPh_4$, **15b** goes to **11b** followed by equilibration with **12b** and subsequent rearrangement to **13b**. Further support for an intermediate such as **15b** is obtained from an in situ study of the reaction of $[\eta^5\text{-}Cp(ON)(OC)Re(PCy_2H)]BF_4$ ((**6b**)BF_4) with $Pt(C_2H_4)_2(PCy_3)$ (in CD_2Cl_2), which occurs as outlined in eq 13.

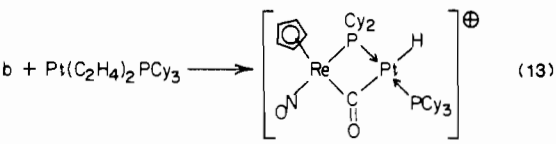

16b (13)

The IR and ^1H and $^{31}P\{^1H\}$ NMR data (Tables I and II) are consistent with initial formation of the bridging- or semibridging-carbonyl species $[Cp(ON)Re(\mu\text{-}PCy_2)(\mu\text{-}CO)PtH(PCy_3)]^+$ (**16b**) (ν(CO) 1800 cm^{-1}; ν(NO) 1733 cm^{-1}). The cation **16b** is structurally similar to the complex $(OC)_3(PEt_3)Mo(\mu\text{-}PPh_2)(\mu\text{-}CO)PtH(PCy_3)$.[5] On standing, **16b** rearranges to the bridging-hydrido platinum carbonyl $[Cp(ON)Re(\mu\text{-}PCy_2)(\mu\text{-}H)Pt(CO)(PCy_3)]^+$ (**17b**) (eq 14). Complex **17b** is structurally

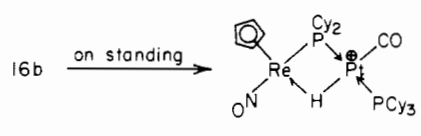

17b (14)

analogous to **11b** and to the complexes $(OC)_4M(\mu\text{-}PCy_2)(\mu\text{-}H)Pt(CO)(PCy_3)$ (M = Cr, Mo, W).[5] Addition of excess PPh_3 to a ca. 4:1 mixture of **11b** and **12b** results in the immediate displacement of CO from platinum and the formation of **9b** and **8b** in a ca. 4:1 ratio, respectively. Addition of excess PPh_3 to **13b** gives **8b** as the sole product.

Characterization of Complexes 7–17. The ^1H and $^{31}P\{^1H\}$ NMR and IR spectra provide ready structural characterization, and the

(11) Chatt, J.; Chini, P. *J. Chem. Soc. A* **1970**, 1538.
(12) Hanckel, J. M.; Darensbourg, M. Y. *J. Am. Chem. Soc.* **1983**, *105*, 6979.
(13) Church, M. J.; Mays, M. J. *J. Chem. Soc. A.* **1968**, 3074.

relevant data for all the new complexes described here are listed in Tables I and II. The relative magnitude of $^1J_{^{195}Pt-^1H}$ and $^2J_{^{31}P(trans\ to\ H)-^1H}$ for the hydride ligand are diagnostic of the bonding mode[2,9,14] being >800 and ca. 165 Hz, respectively, for the platinum terminal hydrides (e.g. **7**, Figure 1a); 400–550 and ca. 55 Hz, respectively, for bridging hydrides (e.g. **9**, Figure 1c); and 30–50 and ca. 0 Hz, respectively, for the rhenium terminal hydrides (e.g. **8**, Figure 1b, and **13b**, Figure 1d). Spin–spin coupling of the platinum hydrido ligand and ^{31}P(cis ligands) is typically 10–25 Hz.[9,14] The $^{31}P\{^1H\}$ NMR data fully support the structures given with $\delta(P_\mu)$ for "$Re(\mu\text{-}PR_2)(\mu\text{-}H)Pt$" and "$\overline{Re(\mu\text{-}PR_2)Pt}$" systems occurring well downfield from the PR_3 resonances while in the singly bridged "$Re(\mu\text{-}PR_2)Pt$" systems (e.g. **7**) $\delta(P_\mu)$ occurs upfield of the PR_3 resonances, consistent with previous literature correlations.[15,16] The $^2J_{^{31}P_\mu-^1H}$ coupling of ca. 30 Hz in the terminal rhenium hydride complexes was confirmed by recording the proton-coupled ^{31}P NMR spectra. The NMR data of $Cp(ON)(OC)Re(\mu\text{-}PCy_2)PtHCl(PPh_3)$ are very similar to those of Trans-$PtHCl(PEt_3)_2$.[17]

The Terminal-Hydride 8 to Bridging-Hydride 9 Isomerization. In CH_2Cl_2 solution the terminal rhenium hydrido cations $[Cp(ON)\overline{HRe(\mu\text{-}PR_2)Pt}(PPh_3)_2]^+$ (**8**) isomerize to the thermodynamically preferred bridging-hydrido structure $[Cp(ON)Re(\mu\text{-}PR_2)(\mu\text{-}H)Pt(PPh_3)_2]^+$ (**9**) (eq 4). Qualitatively, the relative rates for this process are **8c** (μ-PPr_2) > **8a** (μ-PPh_2) ≫ **8b** (μ-PCy_2) with the rate for **8b** being sufficiently slow to allow for the isolation and crystallization of **8b** without contamination with **9b** (on a small scale).

Addition of halide ions (added as $[Ph_3PNPPh_3]^+X^-$) to CH_2Cl_2 solutions of **8b** catalyzes the terminal-hydride to bridging-hydride rearrangement such that isomerization to **9b** is complete in minutes (at ca. 20 °C) as opposed to days/weeks. The reactions are first order in **8b**. The relative rates for the halide- and pseudohalide- (or anion-) promoted **8b** to **9b** rearrangement decrease in the order $N_3^- > Cl^- > SCN^- > Br^- > I^- >>> F^-$ (no effect).[18] However, the difference in rates on varying X^- (excluding F^-) is only an order of magnitude (for $[\mathbf{8b}]_0$ = ca. 5.5×10^{-3} M and $[N_3^-] = 1.93 \times 10^{-3}$ M, $k_{obs} = 10.4\ s^{-1}$; for $[I^-] = 3.91 \times 10^{-3}$ M, $k_{obs} = 1.49\ s^{-1}$ (25 °C)). Reasonable isosbestic points were obtained from the Cl^- and Br^--catalyzed reactions. For I^-, the isosbestic points were less well-defined. A more detailed study of the Cl^- reaction indicated that the isomerization is second order in $[Cl^-]$ (Figure 5) with a rate law of the type $-d[\mathbf{8b}]/dt = k[\mathbf{8b}][Cl^-]^2$ ($k = 1.2 \times 10^6\ M^{-2}\ s^{-1}$ at 25 °C). No long-lived intermediates were observed by IR or NMR spectroscopy. (N.B. In contrast to **7b**, neither **8b** nor **9b** react with an excess of Cl^- to give a neutral species structurally similar to **10b**). Addition of F^-, PPh_3, or pyridine to the Cl^--catalyzed **8b** to **9b** rearrangement did not affect the reaction rate.

Discussion

The oxidative addition of $[Cp(OC)(ON)Re(PR_2H)]^+$ (**6**) to $Pt(C_2H_4)(PPh_3)_2$ gives the (μ-phosphido)platinum hydride $[Cp(ON)(OC)Re(\mu\text{-}PR_2)PtH(PPh_3)_2]^+$ (**7**), a reaction that parallels the formation of $(OC)_5M(\mu\text{-}PPh_2)PtH(PPh_3)_2$ (**2**) from the reaction of $(OC)_5M(PPh_2H)$ with $Pt(C_2H_4)(PPh_3)_2$.[1,5] In contrast, reaction of **6** with $Pt(PPh_3)_4$ leads to rapid loss of CO from Re (a process that thermally is notably difficult in $[Cp(ON)(OC)_2Re]^+$ and $[Cp(ON)(OC)Re(PR_3)]^+$ complexes[8]) and formation of the μ-phosphido terminal rhenium hydride $[Cp(ON)\overline{HRe(\mu\text{-}PR_2)Pt}(PPh_3)_2]^+$ (**8**) as the kinetic product. (Under suitable conditions **7** can rearrange slowly to give **8**.) On standing, **8** isomerizes to the thermodynamically preferred bridging-hydrido cation $[Cp(ON)Re(\mu\text{-}PR_2)(\mu\text{-}H)Pt(PPh_3)_2]^+$ (**9**). Thus the formation of **9** from **7** does not involve a simple substitution of CO from Re nor does it proceed in the manner observed for the formation of $(OC)_4M(\mu\text{-}PPh_2)(\mu\text{-}H)Pt(PPh_3)_2$ (**3**) from $(OC)_5M(\mu\text{-}PPh_2)PtH(PPh_3)_2$ (**2**) (see the preceding paper[5]) since such a process does not account for the intermediacy of **8**. Furthermore the initially formed cis terminal-hydrido platinum cations $[Cp(OC)(ON)Re(\mu\text{-}PR_2)PtH(PPh_3)_2]^+$ (**7**) (in contrast to the neutral analogues $(OC)_5M(\mu\text{-}PPh_2)PtH(PPh_3)_2$ (**2**)) are stable in solution with respect to CO loss for several hours/days at room temperature. However, **7a** and **7b** can be converted to **8** by the addition of proton bases such as F^- and proton sponge (eq 6). When CO transfer from Re to Pt is deliberately forced by taking the neutral hydrido chloro complex $Cp(OC)(ON)Re(\mu\text{-}PCy_2)PtHCl(PPh_3)$ (**10b**) and reacting it with chloride abstracters (eq 9–11), the initial products are an equilibrium mixture of the bridging-hydrido cation $[Cp(ON)Re(\mu\text{-}PCy_2)(\mu\text{-}H)Pt(CO)(PPh_3)]^+$ (**11b**) and the terminal-hydrido rhenium cation $[Cp(ON)\overline{HRe(\mu\text{-}PCy_2)Pt}(CO)(PPh_3)]^+$ (**12b**) in a ratio ca 4:1. This mixture reacts rapidly with PPh_3 to give a ca. 4:1 mixture of **9a** and **8b**. In contrast, the cations **6** react rapidly with $Pt(PPh_3)_4$ to give **8** in >80–95% yield (eq 3). *Consequently, species such as* **11**, **12**, *and* **15** *can be excluded as possible intermediates in the formation of* **8**. The fact that addition of base to the cis terminal platinum hydrido cations **7a** and **7b** facilitates CO loss and formation of **8** and the fact that the most acidic, and hence most easily deprotonated, rhenium diphenylphosphine cation **6a** reacts with $Pt(C_2H_4)(PPh_3)_2$ [less basic than $Pt(PPh_3)_4$] to give both **7a** and **8a** (and **8a** only when the reaction is done in the presence of proton sponge) *points to a deprotonation process being a significant step in the formation of* **8**. Also the *exclusive* and *rapid* formation of **8b** upon addition of PPh_3 to **13b** *suggests that this is probably the CO loss step and points to* **13** *as the immediate precursor in the formation of* **8**. The reaction sequences outlined in Scheme I are proposed as the likely mechanism for the formation of the terminal-hydrido rhenium cations $[Cp(ON)\overline{HRe(\mu\text{-}PR_2)Pt}(PPh_3)_2]^+$ (**8**). Initial deprotonation of **6** by reaction with $Pt(PPh_3)_3$ [N.B. In solution $Pt(PPh_3)_4$ is essentially fully dissociated to $Pt(PPh_3)_3 + PPh_3$[19]] gives the neutral rhenium phosphide $Cp(OC)(ON)Re(PPh_2)$ (**18**) together with the hydrido cation $[PtH(PPh_3)_3]^+$. (N.B. Traces of $[PtH(PPh_3)_3]^+$ are observed in the ^1H NMR spectra on formation of **8** (eq 3).) Complex **18**, which is essentially a phosphine ligand, can then substitute a PPh_3 ligand from either $[PtH(PPh_3)_3]^+$ or $Pt(PPh_3)_3$. The former reaction leads to the cis hydridoplatinum cation **7** (obtained as a minor product). Formation of **7** should be greater for the more basic phosphines **18b** (R = Cy) and **18c** (R = Pr) since **18** and $[PtH(PPh_3)_3]^+$ are likely to be formed in close proximity in the initial oxidative protonation of $Pt(PPh_3)_3$. *The alternative and major reaction of* **18** is with $Pt(PPh_3)_3$ to give initially $Cp(OC)(ON)Re(\mu\text{-}PR_2)Pt(PPh_3)_2$ (**19**) followed by CO transfer to

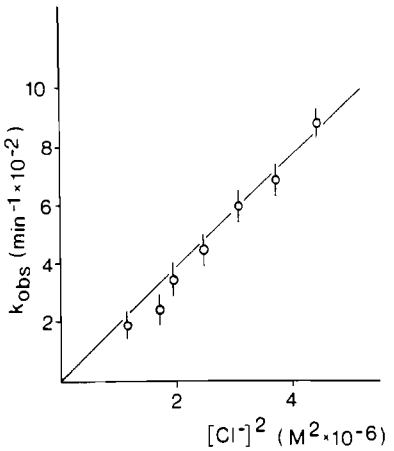

Figure 5. Plot of k_{obs} vs $[Cl^-]^2$ for the Cl^--catalyzed isomerization of $[\eta^5\text{-}Cp(ON)\overline{HRe(\mu\text{-}PCy_2)Pt}(PPh_3)_2]^+$ (**8b**) to $[\eta^5\text{-}Cp(ON)Re(\mu\text{-}PCy_2)(\mu\text{-}H)Pt(PPh_3)_2]^+$ (**9b**) (CH_2Cl_2 solution, 26 °C).

(14) Venanzi, L. M. *Coord. Chem. Rev.* **1982**, *43*, 251.
(15) Carty, A. J. *Adv. Chem. Ser.* **1982**, *No. 196*, 1963.
(16) Garrou, P. E. *Chem. Rev.* **1981**, 229.
(17) Powell, J.; Shaw, B. L. *J. Chem. Soc.* **1965**, 3879.
(18) Kinetic studies of the chloride catalyzed **8b** to **9b** isomerization were limited owing to the difficulties associated with isolating sufficient quantities of **8b** in a pure form.
(19) Malatesta, L.; Cariello, C. *J. Chem. Soc.* **1958**, 2323.

Scheme I. Postulated Mechanisms for the Formation of the Terminal Rhenium Hydrido Cation **8** as the *Major Product* and the Terminal Platinum Hydrido Cations **7** and $[PtH(PPh_3)_3]^+$ as *Minor Products* from the Reaction of $[\eta^5\text{-Cp(OC)(ON)Re(PR}_2\text{H)}]^+$ (**6**) with $Pt(PPh_3)_4$ [$Pt(PPh_3)_3$ + PPh_3 in Solution]

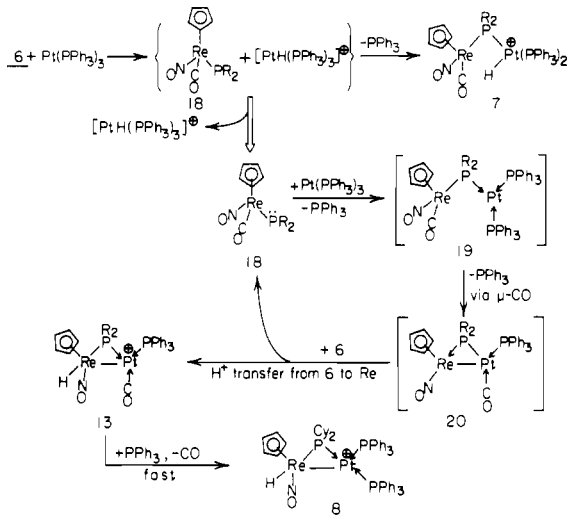

Scheme II. Postulated Mechanisms for Base-Promoted (E.g. F^-) Conversion of **7** to **8**[a]

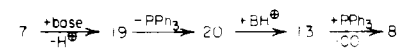

[a] See Scheme I for structures.

Pt to give $Cp(ON)\overline{Re(\mu\text{-}PR_2)}Pt(CO)(PPh_3)$ (**20**). Reprotonation of **20**, using $[Cp(OC)(ON)Re(PR_2H)]^+$ (**6**) as a proton source, gives the thermodynamically preferred hydridorhenium cation $[Cp(ON)H\overline{Re(\mu\text{-}PR_2)}Pt(CO)(PPh_3)]^+$ (**13**) and generates a second molecule of the rhenium phosphide **18** [which then reacts with $Pt(PPh_3)_3$]. Rapid reaction of **13** with PPh_3 leads to $[Cp(ON)H\overline{Re(\mu\text{-}PR_2)}Pt(PPh_3)_2]^+$ (**8**) being formed as the major kinetic product. Our attempts to synthesize the postulated intermediate **20** have been unsuccessful. In seems likely that **20** is a very basic molecule since the cation **13b** does not deprotonate upon addition of proton sponge. Addition of stronger bases such as RLi to **13b** have not lead to isolable products. Indirect evidence in support of the reaction sequences **18** → **13** (Scheme I) comes from the reaction of $[Cp(OC)_3W(PPh_2H)]^+$ (**21**) with $Pt(PPh_3)_4$ to give $Cp(OC)_2\overline{W(\mu\text{-}PPh_2)}Pt(CO)PPh_3$ (**22**) as a readily isolable product according to eq 15.[2] The heterometallic dimer **22**, which

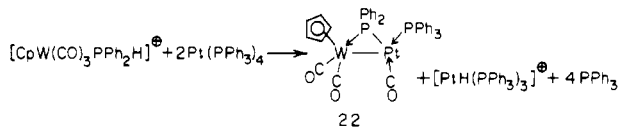

(15)

is structurally analogous to the postulated intermediate **20** (Scheme II) may be protonated by strong acids to give the terminal-hydrido tungsten cation $[Cp(OC)_2H\overline{W(\mu\text{-}PPh_2)}Pt(CO)(PPh_3)]^+$ (**23**) (eq 16), which is structurally similar to **13**. A similar sequence of

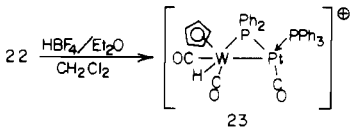

(16)

events accounts for the base-catalyzed rearrangement of the cis hydridoplatinum cations **7a,b** into **8a,b** (see Scheme II).

The proposed mechanism for the formation of 7b,c as the major solution species from the reaction of $[Cp(OC)(ON)Re(PR_2H)]^+$

Scheme III. Postulated Reaction Pathways to Account for the Products Obtained from the Reaction of $[\eta^5\text{-Cp(OC)(ON)Re(PR}_2\text{H)}]^+$ (**6**) with $Pt(C_2H_4)(PPh_3)_2$[a]

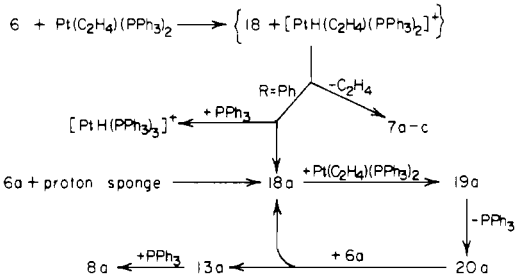

[a] For R = Cy, ^{n}Pr (**6b**, **6c**) the observed products are **7b** and **7c**, respectively. For R = Ph, a mixture of **7a**, **8a**, and $[PtH(PPh_3)_3]^+$ are obtained (see text for details and Scheme I for Structures).

Scheme IV. Postulated Mechanism for the Cl^--Catalyzed Terminal-Hydrido, **8**, to Bridging-Hydrido, **9**, Isomerization

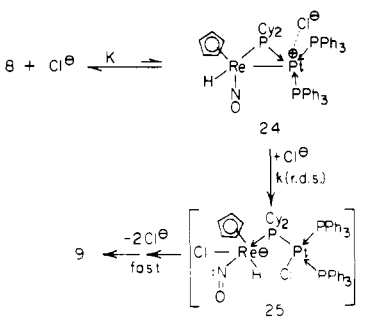

(6b,c) with $Pt(C_2H_4)(PPh_3)_3$ is outlined in Scheme III. Proton transfer from **6b,c** to $Pt(C_2H_4)(PPh_3)_2$ gives $Cp(OC)(ON)Re(PR_2)$ (**18b,c**) and $[PtH(C_2H_4)(PPh_3)_2]^+$ in the close proximity. Rapid displacement of C_2H_4 by the very basic phosphine(s) **18b,c** (R = Cy, Pr) gives **7b,c** as the major product(s). In contrast, reaction of **6a** leads to the less basic and less reactive phosphine $Cp(OC)(ON)Re(PPh_2)$ (**18a**). Consequently the longer lifetime anticipated for **18a** increases its chances of reacting with a $Pt(C_2H_4)(PPh_3)_2$ molecule, which leads to the formation of **8a** as shown. The mechanism outlined in Scheme III also accounts for **8a** being the sole product for the reaction of $[Cp(ON)(OC)Re(PPh_2H)]^+$, proton sponge, and $Pt(C_2H_4)(PPh_3)_2$.

Mechanism of the Halide-Catalyzed 8b to 9b Isomerization. A mechanistic proposal to account for the facile halide-pseudohalide-catalyzed isomerization of the terminal rhenium hydrido cation $[Cp(ON)H\overline{Re(\mu\text{-}PCy_2)}Pt(PPh_3)_2]^+$ (**8b**) to the bridging-hydrido cation $[Cp(ON)Re(\mu\text{-}PCy_2)(\mu\text{-}H)Pt(PPh_3)_2]^+$ (**9b**) is given in Scheme IV. The ineffectiveness of F^- to promote the **8b** to **9b** isomerization and the absence of any effect when F^- or pyridine is added to a Cl^--catalyzed isomerization indicate that the rearrangement does not involve a base-assisted proton transfer (cf. **7** → **8** in Scheme II). The available data point toward a mechanism involving chloride coordination, but without PPh_3 displacement since the reaction is not retarded by the addition of excess PPh_3. We postulate that weak ion pairing of Cl^- at Pt gives the contact ion pair **24**, in low concentration. In the rate-determining step, attack by a second Cl^- at Re generates a short-lived Re(III) "bent nitrosyl" accompanied by loss of the Re–Pt bond to give the "$Re^{III}(\mu\text{-}PCy_2)Pt^{II}$" chloro complex $[Cp(ON)(CO)HClRe(\mu\text{-}PCy_2)PtCl(PPh_3)_2]^-$ (**25**). Subsequent rapid substitution at Pt–Cl by Re–H followed by loss of Cl^- from Re gives the thermodynamically preferred bridging-hydrido isomer **9b**. For low concentrations of **24** and **25**, Scheme IV predicts a rate law of the type $-d[8]/dt = kK[8][Cl^-]^2$. Associative substitution at Re by Cl^- as the rate-determining step in the ReH terminal-to bridging-hydride isomerization is consistent with the qualitative observation that the rate of the **8** to **9** isomerization decreases with increasing "steric size" of the $\mu\text{-}PR_2$ group (i.e. $\mu\text{-}PPr_2 > \mu\text{-}PPh_2 \gg \mu\text{-}PCy_2$).

Table III. Crystal Data, Details of Data Collections[a] and Structure Refinements for $[\eta^5\text{-Cp(ON)HRe}(\mu\text{-PCy}_2)\text{Pt(PPh}_3)_2]\text{PF}_6\cdot 2.5\text{CH}_2\text{Cl}_2$ ((**9b**)PF_6), $[\eta^5\text{-Cp(ON)Re}(\mu\text{-PPh}_2)(\mu\text{-H})\text{Pt(PPh}_3)_2]\text{BF}_4$ ((**9a**)BF_4), and $[\eta^5\text{-Cp(ON)HRe}(\mu\text{-PCy}_2)\text{Pt(PPh}_3)_2]\text{BF}_4\cdot\text{CH}_2\text{Cl}_2$ ((**8b**)BF_4)

	$C_{53}H_{58}F_6NOP_4PtRe\cdot 2.5CH_2Cl_2$ ((**9b**)PF_6)	$C_{53}H_{46}BF_4NOP_3PtRe$ ((**9a**)BF_4)	$C_{53}H_{58}BF_4NOP_3PtRe\cdot CH_2Cl_2$ ((**8b**)BF_4)
system	triclinic	triclinic	monoclinic
a, Å	12.532 (2)	12.563 (2)	11.031 (2)
b, Å	13.077 (2)	12.896 (1)	22.391 (5)
c, Å	19.101 (2)	15.024 (2)	21.603 (7)
α, deg	94.85 (1)	94.14 (1)	90.0
β, deg	105.40 (1)	96.93 (2)	94.04 (2)
γ, deg	91.23 (1)	92.01 (1)	90.0
V, Å^3	3004	2407	5322
Z	2	2	4
fw	1556.5	1273.9	1370.9
space group	$P\bar{1}$	$P\bar{1}$	$P2_1/n$
T, °C	20	20	20
λ, Å	0.71069	0.71069	0.71069
ρ_{calcd}, g cm^{-3}	1.72	1.76	1.71
μ(Mo K$\bar{\alpha}$), cm^{-1}	47.7	56.3	52.9
transm coeff	0.286–0.737 (0.380–0.688)	0.4000–0.664	0.553–0.784
$R(F_o^2)$	0.0471	0.0310	0.0407
$R_w(F_o^2)$	0.0508	0.0325	0.0419

Crystal and Molecular Structures of $[Cp(ON)Re(\mu\text{-PR}_2)(\mu\text{-H})Pt(PPh_3)_2]^+Y^-$ ((9a)Y (R = Ph; $Y^- = BF_4^-$), (9b)Y (R = Cy; $Y^- = PF_6^-$)). Initially, the molecular structure of the μ-hydrido μ-diphenylphosphido cation **9a** (Figure 3) was determined by single-crystal X-ray diffraction (Table III) and has been commented on briefly in a preliminary communication.[3] Since the μ-dicyclohexylphosphido cation **8b** was the only terminal rhenium hydrido cation that could be isolated in a crystalline form suitable for X-ray diffraction studies, we have also determined the molecular structure of its μ-hydrido isomer **9b** (Figure 4) to facilitate an accurate assessment of the structural changes associated with this reorganization. Selected bond lengths and bond angles for the bridging-hydrido cations **9a** and **9b** are given in Table IV. In both structures the geometry at Pt is essentially planar with Pt, Re, the μ-hydride (located for both structures from difference Fourier maps and refined by least-squares), and the three P atoms all lying in the same plane. The immediate coordination geometry at Re, composed of an η^5-C_5H_5, NO, and μ-H can be considered to be pseudooctahedral with η^5-C_5H_5 occupying three coordination sites. The effect of the bulkier cyclohexyl substituents on the μ-phosphido on going from **9a** to **9b** is reflected in *small increases* in the bond distances in the "RePt-μ-P triangle" [by 0.0142 Å (Re–Pt separation), 0.015 Å (Re–μ-P), and 0.030 Å (Pt–μ-P)]. The spacial arrangement of the "$HPtP_3$" fragment in **9a** and **9b**, as determined by the ∠PPtP angles, is very similar to that reported for $[PtH(PPh_3)_3]^+$[20] with ∠PPtP angles between adjacent phosphorus ligands of ca. 100° being reflective of the large steric requirements of these ligands.[21] However a comparison of PtP bond lengths in **9a** and **9b** vs $[PtH(PPh_3)_3]^+$ reveal significant differences between the μ-hydrido and terminal-hydrido cations. In **9a** and **9b** the Pt–P_μ bond length is ca. 0.1 Å shorter than the trans Pt–PPh_3 bond and ca. 0.03 Å shorter than the comparable bond length in $[PtH(PPh_3)_3]^+$. In contrast, the Pt–PPh_3 bond length trans to μ-H (**9a** and **9b**) is shorter by ca. 0.1 Å than the Pt–PPh_3 bond length trans to the terminal H in $[PtH(PPh_3)_3]^+$. This signifies a noticeable decrease in the trans influence of the hydride ligand when in a bridging position[22] and is consistent with the smaller $J_{^{195}Pt-^1H}$ of ca. 420 Hz for the bridging-hydrido cations **9** vis-à-vis the value of ca. 750 Hz for the terminal hydrides in the $[PtH(PR_3)_3]^+$ cations. In **9b**, the hydride bridge is close to symmetrical with Pt–H and Re–H bond lengths of 1.96 (13) and 1.86 (16) Å, respectively. The corresponding bond lengths of 2.20 (6) and 1.57 (6) Å in **9a** suggest a weaker Pt–H interaction in this cation. While the errors in these M–H bond lengths are considerable, it should be noted that these observations are consistent with the lower $J_{^{195}Pt-^1H}$ for **9a** (404 Hz) vs that of **9b** (432 Hz). Other RePt-containing complexes that have been structurally characterized by X-ray diffraction are $Cp(OC)_2HRe$–$PtH(PPh_3)_2$ [Re–Pt 2.838 (1) Å],[23] and $Re_2(CO)_8Pt(Ph_2PCH_2CH_2PPh_2)$[*t*-BuC(O)P].[24]

Table IV. Selected Bond Lengths (Å) and Bond Angles for the Hydrido Cations $[(\eta^5\text{-Cp})(ON)HRe(\mu\text{-PCy}_2)Pt(PPh_3)_2]^+$ (**8b**) and $[(\eta^5\text{-Cp})(ON)Re(\mu\text{-PR}_2)(\mu\text{-H})Pt(PPh_3)_2]$ (**9b**, R = Cy and **9a**, R = Ph)[a]

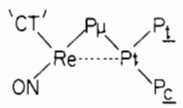

	8b (μ-PCy_2)	**9b** (μ-PCy_2)	**9a** (μ-PPh_2)
Pt–Re	2.8675 (5)	2.8815 (8)	2.8673 (4)
Pt–P_t	2.299 (2)	2.256 (4)	2.269 (2)
Pt–P	2.351 (2)	2.392 (5)	2.361 (2)
Pt–P_μ	2.244 (2)	2.285 (5)	2.255 (2)
Re–P_μ	2.353 (2)	2.355 (4)	3.340 (2)
Re–CT	1.967	1.947	1.937
Re–N	1.741 (9)	1.736 (15)	1.740 (7)
$RePtP_t$	155.85 (6)	155.4 (1)	154.75 (6)
$RePtP_c$	102.28 (6)	105.35 (9)	103.84 (5)
$RePtP_\mu$	53.13 (6)	52.7 (1)	52.73 (1)
P_tPtP_c	101.56 (8)	99.1 (2)	100.74 (8)
P_tPtP_μ	103.19 (8)	103.2 (2)	102.75 (8)
P_cPtP_μ	155.22 (8)	157.5 (1)	156.50 (7)
$PtP_\mu Re$	77.16 (7)	76.8 (2)	77.21 (7)
$PtReP_\mu$	49.71 (5)	50.5 (1)	50.07 (5)
PtReN	91.3 (3)	96.5 (5)	100.0 (2)
PtReCT	121.4	130.9	129.3
P_μReN	96.1 (3)	94.6 (5)	91.9 (3)
P_μReCT	138.0	125.8	123.2
NReCT	125.9	130.0	130.2

[a] CT = the centroid of the η^5-cyclopentadienyl ligand.

Crystal and Molecular Structure of $[Cp(ON)HRe(\mu\text{-PCy}_2)Pt(PPh_3)_2]BF_4$ ((8b)BF_4). An ORTEP drawing of **8b**, giving the atom-labeling scheme, is shown in Figure 2. Relevant bond angles and distances are set out in Table IV. The geometry at Pt in **8b** is essentially planar (Figure 2) and very similar to that observed in **9a** and **9b**. On going from **9b** to **8b**, the major changes in the "$Re(\mu\text{-PCy}_2)Pt(PPh_3)_2$" fragment are (i) a slight decrease of the Pt–Re bond length [2.8815 (8) Å, **9b**; 2.8675 (5) Å, **8b**], (ii) a

(20) Caputo, R. E.; Mak, D. K.; Willett, R. D.; Roundhill, S. G. N.; Roundhill, D. M. *Acta Crystallogr.* **1977**, *B33*, 215.
(21) Clark, H. C.; Hampden-Smith, M. J. *Coord. Chem. Rev.* **1987**, *79*, 229.
(22) Appleton, T. G.; Clark, H. C.; Menzer, L. E. *Coord. Chem. Rev.* **1973**, *10*, 335.
(23) Casey, C. P.; Rutter, E. W., Jr.; Haller, K. J. *J. Am. Chem. Soc.* **1987**, *109*, 6886.
(24) Al-Resayes, S. T.; Hitchcock, P. B.; Nixon, J. F. *J. Chem. Soc., Chem. Commun.* **1987**, 928.

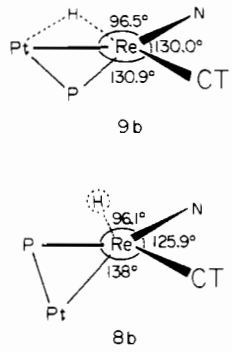

Figure 6. Schematic representation of the major structural differences in **8b** vs **9b** (CT = the centroid of the η^5-Cp ligand).

decrease of the Pt–P_μ bond length by ca. 0.04 Å, (iii) a lengthening of the Pt–PPh_3 distance trans to Re in **8b** by ca. 0.04 Å (trans to μ-H in **9b**), and (iv) a very slight increase in the ∠PPtP angles between adjacent ligands presumably associated with the removal of H from the vicinity of the Pt. The small changes at Pt on going from **9b** to **8b** are similar to those observed for the "Fe(μ-PR_2)Pt(PR'_3)$_2$" fragment on going from $(OC)_3Fe(\mu\text{-}PCy_2)(\mu\text{-}H)Pt(PEt_3)_2$ to $(OC)_3HFe(\mu\text{-}PPh_2)Pt(PPh_3)_2$.[4] In this system, the Pt–Fe bond *does* significantly lengthen by ca. 0.1 Å when there is a μ-hydride bridge as opposed to the terminal-hydride species, and furthermore the change in coordination geometry at Fe that accompanies the bridge to terminal H isomerization is readily discernible. However, in the present complexes, the changes in geometry at Re as the hydride moves from a bridge position, **9**, to a terminal position, **8b**, *are slightly more subtle. These changes are most notable if the geometry at Re is assumed to be pseudotetrahedral using the centroid (CT) of the η^5-cyclopentadienyl ligand as a vertex.* Thus angle changes between **9a** and **9b** at Re are very small (±3°) whereas in **8b** there is a significant increase (+12°) in the angle ∠PReCT, while the remaining pseudotetrahedral angles ∠CTRePt, ∠CTReN, and ∠PtReN decrease by 9, 4, and 5°, respectively, with respect to the angles in **9b** (Table IV). These angle changes have the effect of moving the centroid of the η^5-cyclopentadienyl ring from a position in which it is coplanar with Pt, Re, and N in **9a** and **9b** [$\sum$(angles) = 359.5 (**9a**) and 357.4° (**9b**)] to a position coplanar with P, Re, and N [$\sum$(angles) = 360.0° (**8b**)]. In **8b**, the C_5H_5 and NO groups are moved away from a position cis to the μ-phosphido group (relative to **9a**) suggesting that the H ligand in **8b** is located cis to the phosphido group in a position that is approximately trans to the position of the μ-H ligand in **9b** (see Figure 6). An additional feature that is readily apparent from the data is the significant rotation of the phenyl rings bonded to the PPh_3 cis to Re–Pt in **8b** (Figure 2) so that one of the phenyl rings would appear to block the alternative bridging position for the hydride observable in **9a** and **9b**. Calculation of minimization of the van der Waals repulsion energies for nonbonded atoms between the μ-PCy_2, η^5-C_5H_5, and NO ligands using the structural data for $[Cp(ON)HRe(\mu\text{-}Cy_2)Pt(PPh_3)_2]^+$ (**8b**) (following the procedure of Orpen)[25] reveals a well-defined minimum (in which to locate H) in the region expected. Assuming a terminal Re–H bond length of 1.6–1.7 Å, the data suggest that in **8b** the H ligand is located cis to μ-P, close to or in the "RePPt plane" with a ∠P_μReH of ca 70–75° (Figure 6). Using the extended Hückel molecular orbital method and the fragment orbital formalism,[26] we have carried out calculations on the simplified *neutral* rhenium platinum dimer "η^5-Cp(ON)Re(μ-PH_2)Pt(PH_3)$_2$". The positional parameters for the non-hydrogen atoms were taken from the X-ray structural data for the terminal-hydrido cation $[\eta^5\text{-}Cp(ON)HRe(\mu\text{-}PCy_2)Pt(PPh_3)_2]^+$ (**8b**) and the bridged-hydrido cation $[\eta^5$-Cp(ON)Re(μ-PCy_2)(μ-H)Pt(PPh_3)$_2$]$^+$ (**9b**). Figure 7 shows two-dimensional (in the PtPRe plane) contour diagrams of the HOMO of the model compound η^5-Cp(ON)Re(μ-PH_2)Pt(PH_3)$_2$ produced by using the structural data of the protonated analogues **9b** (Figure 7a) and the structural data of **8b** (Figure 7b). In both examples, the electron density is found to be greatest in the PtPRe plane and in the region where, for the protonated analogues, the proton has been shown to reside (**9b**) or inferred to reside (**8b**).

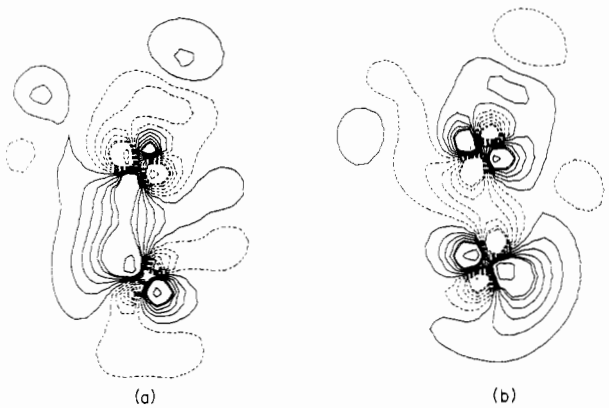

Figure 7. In-plane contour diagrams of the HOMO of the model compound $[\eta^5$-Cp(ON)Re(μ-PH_2)Pt(PH_3)$_2$] calculated[23] (a) by using structural data obtained from the bridging-hydrido rhenium cation **9b** and (b) by using the structural data obtained from the terminal-hydrido cation **8b**.

The question of direct metal–metal bonding in bridged compounds is an area of some controversy and interest with several studies indicating that in doubly bridged systems the major bonding interactions between the two metal atoms may take place through orbitals involving the bridging atoms.[27] The current structural study of the two isomeric hydrides **8b** and **9b** provide additional insight into the nature of metal–metal bonds. Of particular significance are the very small differences in the coordination geometry of the Pt atom on going from **9b** (μ-H) to **8b** (Re–Pt bond). In both cases, the observed ∠PPtP angles are very similar to those observed in $[PtH(PPh_3)_3]^+$[20] and $[PtH(PEt_3)_3]^+$[28] and suggest that removal of H from the bridging position does not markedly effect the electron distribution at Pt. This similarity of structure at Pt (**8b** vs **9b**) is understandable if the Re–Pt bonding in **8b** is considered to be bent, and hence **8b** has a similar spatial distribution of electron density at Pt to that of Pt in the three-center–two-electron H-bridged isomer **9b**. In this description of the bonding, the platinum can be considered to exhibit a valency state of II in *both* **8** and **9** consistent with the planar configuration of the "P_3PtH unit" of (**9**) and that of the "P_3PtRe unit" of **8**. In **8** the RePt interaction is considered to be a "bent metal–metal bond". The observed increase in Pt–P bond length for the PPh_3 ligand trans to μ-H or Re–Pt on going from **9a**/**9b** to **8b** indicates that the bent metal–metal interaction has a greater trans influence than the μ-hydride ligand. In the bridged-hydrido isomer **9** the Re can be considered to be exhibiting a valency state of I while in **8** the Re exhibits a valency state of III. [An alternative description for **8** has Re in a valency state of I together with a bent "Re → Pt" dative bond (effectively a two-electron oxidation at Re).] The advantage of the use of a valency-state formulation is that it accounts for significant changes taking place in the stereochemistry at Re while the coordination geometry at Pt is effectively unchanged. Likewise, on going from

(25) Orpen, A. G. *J. Chem. Soc., Dalton Trans.* **1980**, 2509.
(26) (a) Hoffmann, R. *J. Chem. Phys.* **1963**, *39*, 1397. (b) Hoffmann, R.; Lipscomb, W. *J. Chem. Phys.* **1962**, *37*, 2872.
(27) (a) Benard, M.; Dedieu, A.; Nakamura, S. *Nouv. J. Chim.* **1984**, *8*, 149. (b) Jemmis, E. D.; Pinhas, A. R.; Hoffmann, R. *J. Am. Chem. Soc.* **1980**, *102*, 2576. (c) Bénard, M. *J. Am. Chem. Soc.* **1978**, *100*, 7740. (d) Benard, M. *Inorg. Chem.* **1979**, *18*, 2782. (e) Mason, R.; Mingos, D. M. P. *J. Organomet. Chem.* **1973**, *50*, 53. (f) Summerville, R. H.; Hoffmann, R. *J. Am. Chem. Soc.* **1976**, *98*, 7240. (g) Lauher, J. W.; Elian, M.; Summerville, R. H.; Hoffmann, R. *J. Am. Chem. Soc.* **1976**, *98*, 3219. (h) Churchill, M. R.; Deboer, B. G.; Rotella, F. T. *Inorg. Chem.* **1976**, *15*, 1843.
(28) Russell, D. R.; Mazid, M. A.; Tucker, P. A. *J. Chem. Soc., Dalton Trans.* **1980**, 1737.

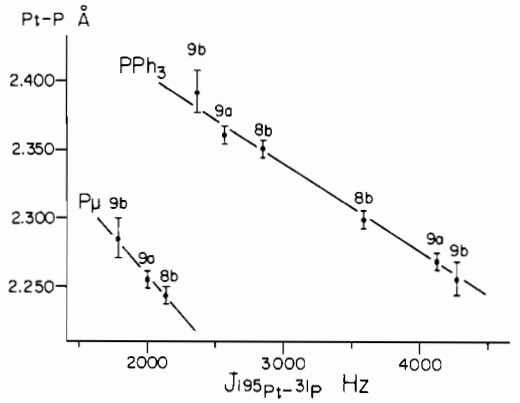

Figure 8. Plot of Pt–P distances vs $^1J_{^{195}Pt-^{31}P}$ for $[\eta^5$-Cp(ON)HRe(μ-PCy$_2$)Pt(PPh$_3$)$_2$]$^+$ (**8b**) and $[\eta^5$-Cp(ON)Re(μ-PR$_2$)(μ-H)Pt(PPh$_3$)$_2$]$^+$ (**9a** (μ-PPh$_2$), **9b** (μ-PCy$_2$)). The error bars are ±3 esd's.

$(OC)_3Fe(\mu\text{-}PCy_2)(\mu\text{-}H)Pt(PEt_3)_2$ to $(OC)_3HFe(\mu\text{-}PPh_2)Pt(PPh_3)_2$, the structural features at Pt are consistent with a valency state of II in both complexes while the observed coordination geometry at Fe is consistent with a change in valency state from 0 (μ-H) to II (terminal H).[4]

Correlation of $J_{^{195}Pt-^{31}P}$ and Pt–P Bond Distance. Several studies have reported a general trend between $^1J_{^{195}Pt-^{31}P}$ and Pt–P bond distances in Pt(II)–phosphine complexes.[29-31] While both parameters are expected to be sensitive to the s-orbital character of the bond, several other molecular variables contribute to the magnitude of $^1J_{^{195}Pt-^{31}P}$[32] and the correlations reported to date are rather poor.[29] In contrast, the Pt–P bond lengths of the structurally similar "PtP$_3$" fragment in the cations **8b**, **9a**, and **9c** (Table IV) correlate well with $^1J_{^{195}Pt-^{31}P}$ data with longer Pt–P bonds being associated with a decrease in J (Figure 8). This observation is understandable if the variation in coupling in these cations is reflective of changes in s-orbital overlap. Particularly noteworthy is the observation that, for a comparable bond length, $^1J_{^{195}Pt-^{31}P_\mu}$ for **8** and **9** is less than 50% that of $^1J_{^{195}Pt-^{31}PPh_3}$. This suggests decreased s-orbital contribution to the P$_\mu$–Pt bond even though the bond is shorter presumably due to ring-strain effects (N.B. $\angle ReP_\mu Pt \sim 77°$). In contrast, $^1J_{^{195}Pt-^{31}P_\mu}$ for $[\eta^5$-Cp(OC)(ON)Re(μ-PR$_2$)PtH(PPh$_3$)$_2$]$^+$ (**7**) ($\angle RePPt$ presumed to be >100°) is very similar in magnitude to that of the PPh$_3$ ligand trans to P$_\mu$ (Table II). On going from **7** to **9**, trans $^2J_{^{31}P_\mu-^{31}P}$ coupling decreased from ca. 300 to ca. 215 Hz, consistent with decreased s-character in the P$_\mu$ bond of **9**. The fact that the Pt–P$_\mu$ bond lengths are consistently shorter than Pt–PPh$_3$ (trans to P$_\mu$) bond lengths by ca. 0.1 Å may also be reflective of "ring strain". The decrease in P–P bond length from a normal value of 2.27 Å to a value of 2.20 Å in the strained molecule P$_4$ has been ascribed to bent P–P σ-bonding.[33]

Experimental Section

General Data. All manipulations were carried out under an atmosphere of dry N$_2$ or argon, using dry and degassed solvents. IR spectra (CH_2Cl_2 solution) were recorded on a Nicolet 10DX spectrometer. ^1H and $^{31}P\{^1H\}$ NMR spectra (CD_2Cl_2 solution) were obtained on a Varian XL200 spectrometer, and chemical shifts were referenced to tetramethylsilane and 85% H_3PO_4, respectively. Microanalyses were carried out by Canadian Microanalytical Laboratories.

Starting Materials. $[(\eta^5$-Cp)Re(CO)$_2$(NO)]BF$_4$ and $[(\eta^5$-Cp)Re(CO)(NO)(MeCN)]BF$_4$ were prepared by the method of Tam et al.[8] Re$_2$(CO)$_{10}$ was purchased from Pressure Chemical Co. PPh_2H, PCy_2H, and P^nPr_2H were purchased from either Pressure or Strem Chemical Inc. [NO]BF$_4$, [Ph$_3$PNPPh$_3$]Cl, [Et$_4$N]Cl, NaBF$_4$, NaBPh$_4$, and NaPF$_6$ were purchased from Aldrich Chemical. Pt(C$_2$H$_4$)(PPh$_3$)$_2$,[34] Pt(PPh$_3$)$_4$,[35] and Pt(C$_2$H$_4$)$_2$(PCy$_3$)[36] were prepared by literature methods.

$[(\eta^5$-Cp)Re(CO)(NO)(PPh$_2$H)]BF$_4$ ((**6a**)BF$_4$) was prepared from the reaction of $[(\eta^5$-Cp)Re(CO)(NO)(MeCN)]BF$_4$ with PPh_2H in THF according to the method described by Tam et al.[8] for preparation of $[(\eta^5$-Cp)Re(CO)(NO)(PPh$_3$)]BF$_4$. Yellow air-stable crystals of (**6a**)BF$_4$ were recrystallized from CH_2Cl_2/ether (80% yield). Data: IR (cm^{-1}, CH_2Cl_2) ν(CO) 2029 (s), ν(NO) 1760 (s); ^1H NMR (CD_2Cl_2) δ 8.02 (1 H, d, $J_{^{31}P-^1H}$ = 428 Hz, P*H*), 7.47 (10 H, m, C$_6H_5$), 6.01 (5 H, s, η^5-C$_5H_5$). Anal. Calcd for $C_{18}H_{16}BF_4NO_2PRe$: C, 37.13; H, 2.77; N, 2.41; P, 5.32. Found: C, 36.80; H, 2.39; N, 2.42; P, 5.25.

$[(\eta^5$-Cp)Re(CO)(NO)(PCy$_2$H)]BPh$_4$ ((**6b**)BPh$_4$) and $[(\eta^5$-C$_5$H$_5$)Re(CO)(NO)(P^{n}Pr$_2$H)]BPh$_4$ ((**6c**)BPh$_4$) were prepared in a manner directly analogous to that used for (**6a**)BF$_4$. However the BPh$_4^-$ salts of **6b** and **6c** proved considerably more tractable than the corresponding BF$_4^-$ salts. (**6b**)BPh$_4$ and (**6c**)BPh$_4$ were precipitated from ethanol solutions of the BF$_4^-$ salts by addition of NaBPh$_4$ and recrystallized from CH_2Cl_2/ether (yields 40–60%). Data for (**6b**)BPh$_4$ (yellow crystals): IR (cm^{-1}, CH_2Cl_2) ν(CO) 2018 (s), ν(NO) 1763 (s). ^1H NMR (CD_2Cl_2) δ 7.34, 7.04, 6.90 (8, 8, 4 H; m, m, m; C$_6H_5$), 5.41 (5 H, d, $J_{^{31}P-^1H}$ = 0.6 Hz, C$_5H_5$), 5.03 (1 H, d of t, $J_{^{31}P-^1H}$ = 375 Hz, $J_{^1H-^1H}$ = 5 Hz, P*H*), 2.21–1.32 (22 H, m, C$_6H_{11}$). Anal. Calcd for $C_{42}H_{48}BNO_2PRe$: C, 61.01; H, 5.85; N, 1.69. Found: C, 60.64; H, 5.72; N, 1.73. Data for (**6c**)BPh$_4$ (yellow crystals): IR (cm^{-1}, CH_2Cl_2) ν(CO) 2021 (s), ν(NO) 1766 (s); ^1H NMR (CD_2Cl_2) δ 7.35, 7.05, 6.91 (8, 8, 4 H; m, m, m; C$_6H_5$) 5.33 (5 H, d, $J_{^{31}P-^1H}$ = 0.6 Hz, C$_5H_5$), 5.14 (1 H, d of quin, $J_{^{31}P-^1H}$ = 392 Hz, $J_{^1H-^1H}$ = 6 Hz, P*H*), 1.93 (4 H, m, PC*H*$_2$CH$_2$CH$_3$), 1.46 (4 H, m, PCH$_2$*CH*$_2$CH$_3$), 1.09 (6 H, t, J = 7 Hz, C*H*$_3$). Anal. Calcd. for $C_{36}H_{40}BNO_2PRe$: C, 57.91; H, 5.40; N, 1.88. Found: C, 57.83; H, 5.38; N, 1.90.

Reactions of 6a–c with Pt(C$_2$H$_4$)(PPh$_3$)$_2$, Pt(PPh$_3$)$_4$, and Pt(C$_2$H$_4$)$_2$(PCy$_3$). The course of the reactions of **6a–c** with Pt(0) complexes were studied by IR and NMR spectroscopy. In a typical IR experiment, to 0.05 g of **6a**, dissolved in 10 mL of CH_2Cl_2 in a 100-mL flask was added with stirring 0.064 g Pt(C$_2$H$_4$)(PPh$_3$)$_2$ and the reaction monitored by IR spectroscopy (carbonyl region) by periodic sampling of the reaction mixture using 0.1-cm NaCl or CaF$_2$ IR cells. NMR experiments were carried out either by mixing the reactants directly in the NMR tube followed by addition of CD_2Cl_2 or by carrying out the reaction in CH_2Cl_2 on a scale similar to that in the IR experiment above where, after the desired reaction time, the solvent was removed in vacuo and the residue redissolved in CD_2Cl_2 and its NMR spectrum recorded.

$[(\eta^5$-Cp)(ON)HRe(μ-PCy$_2$)Pt(PPh$_3$)$_2$]BPh$_4$ ((**8b**)BPh$_4$). Pt(PPh$_3$)$_4$ (0.295 g) was added to a solution of **6b** (0.205 g) in 20 mL of CH_2Cl_2. The mixture was stirred for 4 h and chromatographed on a silica gel column (15 cm) eluting with CH_2Cl_2. The elute was concentrated and the golden yellow product precipitated by addition of hexane. The crude product (0.27 g, 72% yield) always contained a small amount of the bridged hydride isomer **9b**, and although purity was generally >95%, as judged by IR spectroscopy, attempts to obtain **8b** pure in amounts any greater than that required for an X-ray structure determination (a few crystals) were unsuccessful.

$[\eta^5$-Cp(ON)Re(μ-PPh$_2$)(μ-H)Pt(PPh$_3$)$_2$]BF$_4$ ((**9a**)BF$_4$). Pt(PPh$_3$)$_4$ (0.310 g) was added to a solution of **6a** (0.145 g) in 20 mL of acetone. The mixture was stirred for 1 h, and ca. 0.1 g of [Ph$_3$PNPPh$_3$]Cl was added. After being stirred for a further 1 h, the mixture was concentrated and cooled to give red crystals, which were isolated by filtration and washed with cold acetone. Yield of (**9a**)BF$_4$: 0.246 g, 78%. Anal. Calcd for $C_{53}H_{46}BF_4NOP_3PtRe$: C, 49.97; H, 3.64; N, 1.10. Found: C, 49.97; H, 3.63; N, 1.06.

$[(\eta^5$-Cp)(ON)Re(μ-PCy$_2$)(μ-H)Pt(PPh$_3$)$_2$]BPh$_4$ ((**9b**)BPh$_4$). To a CH_2Cl_2 solution containing (**8b**)BPh$_4$ (prepared as described above) was added 0.1 g or [Ph$_3$PNPPh$_3$]Cl. After the mixture was stirred for 1 h, the solvent was removed in vacuo and the residue chromatographed on silica gel eluting with CH_2Cl_2. The solution was concentrated and hexane added to precipitate (**9b**)BPh$_4$ as a yellow-gold powder, which was isolated by filtration, washed with hexane, and dried in vacuo. Yield: 73% (based on **6b**). Anal. Calcd for $C_{77}H_{78}BNOP_3PtRe$: C, 60.91; H, 5.18; N, 0.92. Found: C, 60.72; H, 5.46; N, 0.89.

$[(\eta^5$-Cp)(ON)Re(μ-P^{n}Pr$_2$)(μ-H)Pt(PPh$_3$)$_2$]BPh$_4$ ((**9c**)BPh$_4$) was prepared from (**6c**)BPh$_4$ and Pt(PPh$_3$)$_4$ by the method described above for (**9a**)BF$_4$. Yield: 57%. Anal. Calcd for $C_{71}H_{70}BNOP_3PtRe$: C, 59.29; H, 4.91; N, 0.97. Found: C, 58.85; H, 5.04; N, 0.92.

$[\eta^5$-Cp(ON)(OC)Re(μ-PCy$_2$)PtHCl(PPh$_3$)] (**10b**). Pt(C$_2$H$_4$)(PPh$_3$)$_2$ (0.044 g) was added to (**6b**)BPh$_4$ (0.048 g) dissolved in 10 mL of CH_2Cl_2. After the mixture was stirred for 5 min, [AsPh$_4$]Cl (0.027 g) was added.

(29) Bao, Q.-B.; Geib, S. J.; Rheingold, A. L.; Brill, T. B. *Inorg. Chem.* **1987**, *26*, 3453.
(30) Mather, G. G.; Pidcock, A.; Rapsey, G. J. N. *J. Chem. Soc., Dalton Trans.* **1973**, 2095.
(31) Pidcock, A. *Adv. Chem. Ser.* **1982**, *No. 196*, 1.
(32) Pople, J. A.; Santry, D. P. *Mol. Phys.* **1964**, *8*, 1.
(33) Hilliar, I. A.; Saimders, V. R. *Chem. Commun.* **1970**, 1233.
(34) Blake, D. M.; Roundhill, D. M. *Inorg. Synth.* **1978**, *18*, 120.
(35) Ugo, R.; Cariati, F.; LeMonica, G. *Inorg. Synth.* **1968**, *11*, 105.
(36) Spencer, J. L. *Inorg. Synth.* **1979**, *19*, 216.

The reaction mixture was stirred for 15 min and then the solvent removed under vacuum. The residue was extracted with 15 mL of benzene, filtered, and concentrated under vacuum and hexane added to precipitate **10b** as a bright yellow solid, which was collected by filtration, washed with hexane, and dried under vacuum. Yield: 0.036 g, 62%. Anal. Calcd for $C_{36}H_{43}ClNO_2P_2PtRe$: C, 43.22; H, 4.33; N, 1.40. Found: C, 42.54; H, 4.12; N, 1.36.

Reactions of 10b with $AgBF_4$ and $NaBPh_4$. (i) $NaBPh_4$ (0.048 g) was added to **10b** (0.110 g) dissolved in 10 mL of acetone. Solvent was removed under vacuum. The residue was dried under vacuum for 10 min and dissolved in 10 mL of CH_2Cl_2, and the solution was monitored by IR spectroscopy.

(ii) **10b** (0.120 g) was dissolved in 10 mL of CH_2Cl_2. Excess $AgBF_4$ was added and the reaction stirred for 30 min. After filtration, the solvent was removed under vacuum and the residue redissolved in CD_2Cl_2 for ^1H and ^{31}P NMR spectroscopy.

X-ray Crystallography. The BPh_4^- salts of **8b** and **9b** gave poor-quality crystals. Crystals of the BF_4^- salt of **8b** were grown by slow diffusion of hexane into a CH_2Cl_2 solution. Crystals of the BF_4^- salt of **9b** rapidly lost solvent of crystallization. However the PF_6^- salt proved to be more stable to solvent loss and crystals were sealed in 0.2–0.3-mm Lindemann capillaries with a small amount of mother liquor. Anion exchange was carried out by addition of a CH_2Cl_2 solution of $[Et_4N]BF_4$ or $[Et_4N]PF_6$ to a CH_2Cl_2 solution of the BPh_4^- salt of **8b** and **9b**. Precipitation of $[Et_4N]BPh_4$, which is sparingly soluble in CH_2Cl_2, followed by filtration gave a solution with the desired counterion from which suitable crystals were obtained. Relevant experimental details are summarized in Table III. Final atomic positional parameters and complete listings of bond lengths and bond angles have been deposited.

Calculations of van der Waals repulsion energies in the region between the μ-PCy_2, NO, and η^5-C_5H_5 ligands of **8b** were carried out by using the CHEM-X program (Chemical Design Ltd., Oxford, U.K.) following the approach of Orpen for the indirect location of hydride ligands in metal clusters.[25] The program uses a Buckingham potential of the form

$$V(r) = \frac{a \exp(-br)}{r^d} - \frac{c}{r^6}$$

The parameters *a–d* for various atoms are those reported by Orpen. The Re–H bond length was fixed at 1.6 Å, and positional parameters for the non-hydrogen atoms were taken from the X-ray structural data for **8b**. The hydrogen atoms were positioned by the program with C–H bond lengths of 1.00 Å. Computation of energy maps in the RePPt plane and at positions ±5 and ±10° out of this plane indicated a distinct energy minimum suitable for the location of a hydride ligand close to or in the RePPt plane (±0.2 Å) with a ∠PReH of 70–75°.

EHMO calculations were carried out on the simplified complex $[\eta^5$-$Cp(ON)Re(\mu$-$PH_2)Pt(PH_3)_2]$ with non-hydrogen interatomic distances based on the X-ray crystal structures of **8b** and **9b** with P–H = 1.40 Å and ∠Pt–P–H = 110°. Values for H_{ii} and orbital exponents were taken from ref 37.

Acknowledgment. We are grateful to the Natural Sciences and Engineering Research Council of Canada for financial support of this research.

Registry No. (**6a**)BF_4, 123125-34-8; (**6b**)BF_4, 123125-39-3; (**6b**)BPh_4, 123125-36-0; (**6c**)BF_4, 123125-40-6; (**6c**)BPh_4, 123125-38-2; (**7a**)BF_4, 123125-51-9; (**7b**)BPh_4, 123166-12-1; (**7c**)BPh_4, 123125-53-1; (**8a**)BF_4, 123125-55-3; (**8b**)BF_4, 123125-47-3; (**8b**)BF_4·CH_2Cl_2, 123125-48-4; (**8b**)BPh_4, 123125-41-7; (**8c**)BPh_4, 123125-57-5; (**9a**)BF_4, 101332-90-5; (**9b**)BPh_4, 123125-42-8; (**9b**)PF_6, 123125-45-1; (**9b**)PF_6·$2.5CH_2Cl_2$, 123125-46-2; (**9c**)BPh_4, 123125-44-0; **10b**, 101307-86-2; (**11b**)BPh_4, 123166-13-2; (**12b**)BPh_4, 123166-14-3; (**13b**)BPh_4, 123166-15-4; **14b**, 123125-62-2; **15b**, 101923-29-9; (**16b**)BPh_4, 123125-59-7; (**17b**)BPh_4, 123125-61-1; $[(\eta^5$-$Cp)Re(CO)(NO)(MeCN)]BF_4$, 92269-93-7; PPh_2H, 829-85-6; PCy_2H, 829-84-5; P^nPr_2H, 19357-87-0; $Pt(C_2H_4)(PPh_3)_2$, 12120-15-9; $Pt(PPh_3)_4$, 14221-02-4; $Pt(C_2H_4)_2(PCy_3)$, 57158-83-5; $[\eta^5$-$Cp(ON)Re(\mu$-$PH_2)Pt(PH_3)_2]$, 123125-49-5; $Pt(CO)_2(PPh_3)_2$, 15377-00-1.

Supplementary Material Available: Examples of first-order rate plots [ln $(A - A_\infty)$ vs t] and plots of spectroscopic changes, ν(NO) region, for the Cl^--catalyzed **8b** to **9b** isomerization and, for compounds (**8b**)BF_4, (**9a**)BF_4, and (**9b**)PF_6, tables of structure determination data, positional and thermal parameters, and complete bond lengths and bond angles (30 pages); tables of final structure factor amplitudes (87 pages). Ordering information is given on any current masthead page.

(37) Summerville, R. H.; Hoffmann, R. *J. Am. Chem. Soc.* **1976**, *98*, 7240.

Contribution from the Department of Chemistry,
University of Toronto, Toronto, Ontario, Canada M5S 1A1

Synthesis of "$PtRu_2$" and "$PtRu_3$" Heterometallic Complexes from the Reaction of $Ru_3(CO)_{11}(PPh_2H)$ with Zerovalent Complexes of Platinum. Single-Crystal X-ray Diffraction Studies of $PtRu_2(\mu$-$PPh_2)(\mu$-$H)(CO)_7(PCy_3)$ and $PtRu_3(\mu$-$PPh_2)(\mu$-$H)(CO)_9(PCy_3)$

John Powell,* John C. Brewer, Giulia Gulia, and Jeffery F. Sawyer

Received November 30, 1988

The reaction of $Ru_3(CO)_{11}(PPh_2H)$ (**4**) with $Pt(C_2H_4)(PPh_3)_2$ gives $PtRu_2(\mu$-$PPh_2)(\mu$-$H)(CO)_7(PPh_3)$ (**6a**) and $Pt_2Ru(CO)_5(PPh_3)_3$ (**7**) as the major products. The reaction of **4** with $Pt(C_2H_4)_2(PCy_3)$ gives $PtRu_2(\mu$-$PPh_2)(\mu$-$H)(CO)_7(PCy_3)$ (**6b**) and $PtRu_3(\mu$-$PPh_2)(\mu$-$H)(CO)_9(PCy_3)$ (**8**) as the major products together with several minor "Ru_xPt_y" species. The molecular structures of **6b** and **8** have been determined by single-crystal X-ray diffraction. Crystal data for **6b**: $C_{37}H_{44}O_7P_2PtRu_2$ crystallizes in space group $P2_1/n$ with a = 13.075 (5) Å, b 20.576 (4) Å, c = 15.316 (7) Å, β = 102.38 (3)°, V = 4025 Å^3, and D_x = 1.75 g cm^{-3} for Z = 4; R (R_w) = 0.0324 (0.0327) for 5932 observed data [$I \geq 3\sigma(I)$]. Crystal data for **8**: $C_{45}H_{56}O_9P_2PtRu_3$·CH_2Cl_2 crystallizes in space group $P2_1/c$ with a = 9.605 (3) Å, b = 23.713 (12) Å, c = 20.600 (5) Å, β = 95.76 (2)°, V = 4668 Å^3, and D_x = 1.77 g cm^{-3} for Z = 4; R (R_w) = 0.0605 (0.0645) for 3954 observed data [$I \geq 3\sigma(I)$]. Complex **6b** contains a $PtRu_2$ triangle with one direct PtRu and one direct RuRu metal–metal bond. The hydride bridges a PtRu edge while the μ-PPh_2 ligand bridges the RuRu edge such that the RuPRu plane is approximately orthogonal to the $PtRu_2$ plane. The structure of **8** is formally derived from that of **6b** by the addition of a "$Ru(CO)_2$" moiety to **6b** along a line bisecting the Ru–Ru bond and passing through P_μ of the PPh_2 group such that the resulting structure essentially consists of a square-planar $(Cy_3P)(OC)Pt(H)(Ru2)$ center linked by the μ-H and Pt–Ru2 metal–metal bonds to a $Ru_3(\mu$-$CO)_2(\mu$-$PPh_2)(CO)_6$ planar moiety. In **6b**, the bridging hydrogen atom was located and refined such that Pt–H_μ = 1.65 (4) Å, Ru1–H_μ = 1.66 (4) Å, and $PtH_\mu Ru1$ = 121 (3)°.

Introduction

The oxidative addition of the P–H bond of a secondary phosphine complex to zerovalent phosphine complexes of platinum is a simple and effective means of incorporating a single bridging-phosphido group into a range of "MPt", "MPt_2", and "MPt_3" complexes.[1-5] Typically, complexes of the type $(OC)_xM(PR_2H)$ (M = Cr, Mo, W, x = 5; M = Fe, Ru, x = 4)[1,4] and cationic

(1) Powell, J.; Gregg, M. R.; Sawyer, J. F. *J. Chem. Soc., Chem. Commun.* **1984**, 1149.

0020-1669/89/1328-4470$01.50/0 © 1989 American Chemical Society